

An Integrated Approach For Digital Image Inpainting

Lavina Kalra

PG Student, Department of CSE
NITTTR, Chandigarh, India

Dr. Maitreyee Dutta

Professor and Head, Department of ECE
NITTTR, Chandigarh, India

Abstract— In this paper, we present an efficient integrated approach for digital image inpainting of coloured images. The approach makes use of adaptive Wiener filtering of each component channel of the mask image at the first step to remove any unwanted noise from the image. The filtered image has better clarity in terms of the mask area to be inpainted and is further used to inpaint the input image using classic exemplar inpainting approach as the second step. The output obtained is compared to a reference image to find how closely it resembles the reference image. The performance of this approach is presented both in terms of visual results and quantitative parameters like peak signal to noise ratio (PSNR), mean squared error (MSE) and execution time (in seconds). Images can easily be manipulated, scaled up or down, objects can be deleted from scenes, background extracted, special effects introduced and many more applications carried out by the help of this approach without compromising on the performance of inpainting. The experimental results obtained are furthermore compared to the latest state of the art techniques in the area of inpainting so as to prove the competitiveness, effectiveness and efficiency of this approach.

Index terms - Image Inpainting, Object Removal, Image Reconstruction, Image Restoration.

I. INTRODUCTION

Image inpainting is not just scientific technique but also an art that enables the reconstruction of missing areas in a seamless manner. It has always been a difficult and time consuming yet essential task to reconstruct images manually like in the case of excavated distorted paintings, papers, maps, in special effects, etc [15]. But with the advancements in science and the digitization of media this field of inpainting is gaining momentum. It has become possible to regain missing portions of digital images without huge investments of effort and time through image inpainting – a process that reproduces the distorted and otherwise lost parts of an image by the help of image processing techniques. It is thus a technique using which images can be manipulated in order to enhance their utility for various purposes. It is widely used in areas of reconstruction of scratched old photographs and old movies, text extraction from images, digital zooming [13] and to insert or eliminate objects in the scenes to produce optical illusions and special effects [16].

Inpainting approaches take a distorted image as input and processes it to produce an image that is free of distortions. The main objective behind any inpainting algorithm is to fill-up the missing regions and cracks using the available information from the surrounding environment. Hence it finds use in numerous fields, like the restoration of classic films and artworks [24], obtaining improved compression ratios [23],

providing special effects in digital media, background extraction, object removal, etc. Figure 1 shows the basic concept of inpainting.

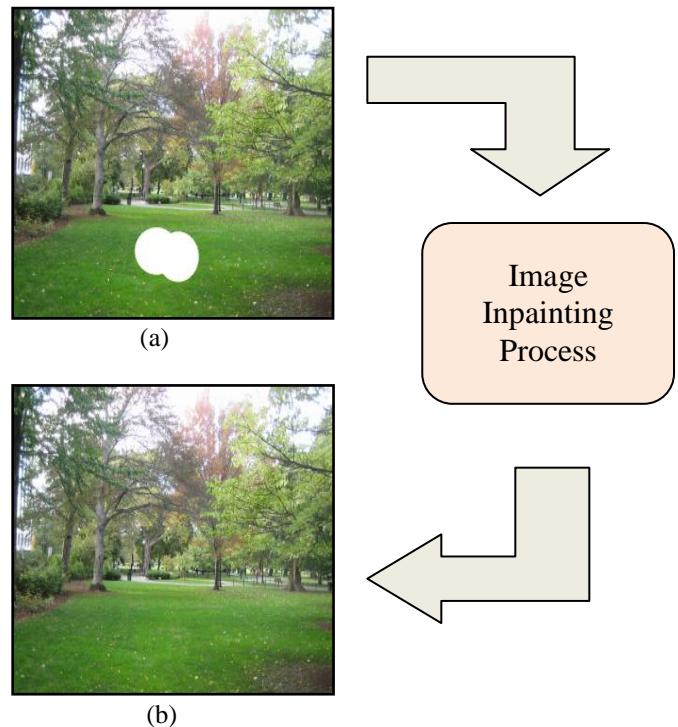


Figure 1. An example of Image Inpainting. (a) The input image with marked area to be inpainted. (b) The inpainted image.

Inpainting approaches take a distorted image as input and processes it to produce an image that is free of distortions. The main objective behind any inpainting algorithm is to fill-up the missing regions and cracks using the available information from the surrounding environment. Hence it finds use in numerous fields, like the restoration of classic films and artworks [24], obtaining improved compression ratios [23], providing special effects in digital media, background extraction, object removal, etc. Figure 1 shows the basic concept of inpainting.

II. RELATED WORK

Bertalmio et.al [1], the pioneers in the field of image inpainting proposed a method that attempted to restore the lost regions of damaged images by diffusion of information. The

information gets diffused from the respective exterior areas of the missing portions alongside the application of partial differential equations at the edges of the corrupt area. It was followed by the formulation of Total Variational (TV) model by Chan and Shen [2][3]. Euler Lagrange equation was designed for inpainting smaller regions and proved efficient for noise removal, but broken edges could not be repaired. The extension of TV algorithm, Curvature-Driven Diffusion (CDD) model [6] was aimed at obtaining the broken connectivity. Similar to the TV model and Bertalmio et al's model, [5] and [19] too rely on partial differential equations. These techniques were focused towards use of structural properties and partial differential equations to obtain the missing areas. Vahid Bastani [23] proposed an algorithm for image compression that was based on an image inpainting system. The regions in the image capable of being precisely restored are located and their data is extracted. The remaining portions' information is encoded to give output. At the decoder end, an inpainting method that is based upon the use of partial differential equations is applied to recover the entire image. Tensor based reconstruction [9] works on the concept of propagating the information about the structure to the target areas. The paper proposed three algorithms- SiLTRC, FaLTRC, HaLTRC i.e. Simple Low Rank Tensor Completion, Fast Low Rank Tensor Completion and High Accuracy Low Rank Tensor Completion and compared the three. HaLTRC is found to be the best one and has been referred to in this paper for comparison of performance.

Apart from this class of algorithms, a new class of inpainting algorithms emerged that was based on texture synthesis. Igehy and Pereira [7] proposed use of the texture synthesis method in their algorithm to inpaint the distorted region. The regions of unknown texture were painted using the texture from other known regions. Texture synthesis approach is highly useful in images where there is some kind of structure and uniformity in the texture of the image [8], [20]. However, it is not so efficient for images which require replacing areas with not much adherence to a specific texture.

Following this development, researchers tried to combine the benefits of both the approaches into one. So a Hybrid class of inpainting algorithms rose. Bertalmio et al. [17] introduced the idea of decomposing the image into separate parts so that structure and texture inpainting can be used simultaneously to regain the target area. Revolving about the same idea a number of algorithms developed like Li et al [12] proposed an algorithm that uses compressed sensing (CS) in the frequency domain in order to recover damaged images. The image is disintegrated into two functions - structure and textual parts. The method ensured a decent restoration of the structure and quality of the image. Xu and Wang [22] also used the same concept and decomposed the input image using wavelet transformation into structure and texture parts and used TV Model and Texture Synthesis on these parts respectively. It could inpaint the missing parts but the image contrast was poor and also the image got blurred.

Criminisi et al [4] provided an algorithm that could remove considerably larger objects from images. The algorithm used exemplar-based texture synthesis which was modulated by a unified approach to decide the sequence of filling target areas. Following this algorithm, a number of other techniques surfaced like [20] and [21] and even the latest research in the field of inpainting is taking place considering exemplar based method as their core. Guillemot et al [11] presented an exemplar-based inpainting technique based on a locally linear embedding algorithm with a low-dimensional neighborhood representation (LLE-LDNR). The technique initially locates the K nearest neighbors (K-NN) to be inpainted and linearly combines them with LLE-LDNR to recover the unknown pixels values.

Exemplar inpainting was also the basis of the technique formulated in [18]. It used higher order singular value decomposition for stack of candidate patches and finally inverted the transform and took weighted average of the same which yielded a filtered patch that is used to find the target patch. It produces excellent image quality and has been used for comparison with our work in this paper.

All the above processes for inpainting can be categorized into three main types [14]: Structure-based inpainting, Texture-synthesis and Hybrid inpainting [17] [25]. Structure-based inpainting is the process of inpainting which uses the information around target region to estimate isophotes [1][9]. They perform in an excellent manner on small-scale but they tend to blur when inpainting comparatively large damaged regions. Texture-synthesis inpainting [7] is the filling up of missing information with the help of texture synthesis techniques and is appropriate for inpainting relatively larger damaged regions where texture is somewhat uniform [18]. Certain algorithms employ a combination of both the above mentioned techniques to inpaint the images by addressing both the components. These kind of algorithms fall into the category of Hybrid Inpainting [17] methods.

III. PROPOSED APPROACH

In this paper we have introduced an adaptive filtering step before carrying out the actual inpainting as is shown in the flowchart in Figure 2. It improves the mask processing of the inpainting approach.

The improved algorithm uses three images as input-

- a) The image that needs to be inpainted
- b) The image that demarcates the mask
- c) Reference image

The reference image is not used for inpainting but only for the computation of final results. Mostly algorithms like in [4], [9], [10] and [18] carry out inpainting on the input image without having any reference image to compare the results with. This is called Blind Inpainting.

To obtain comparison in visual and quality metrics we have used a separate reference image.

Flowchart:

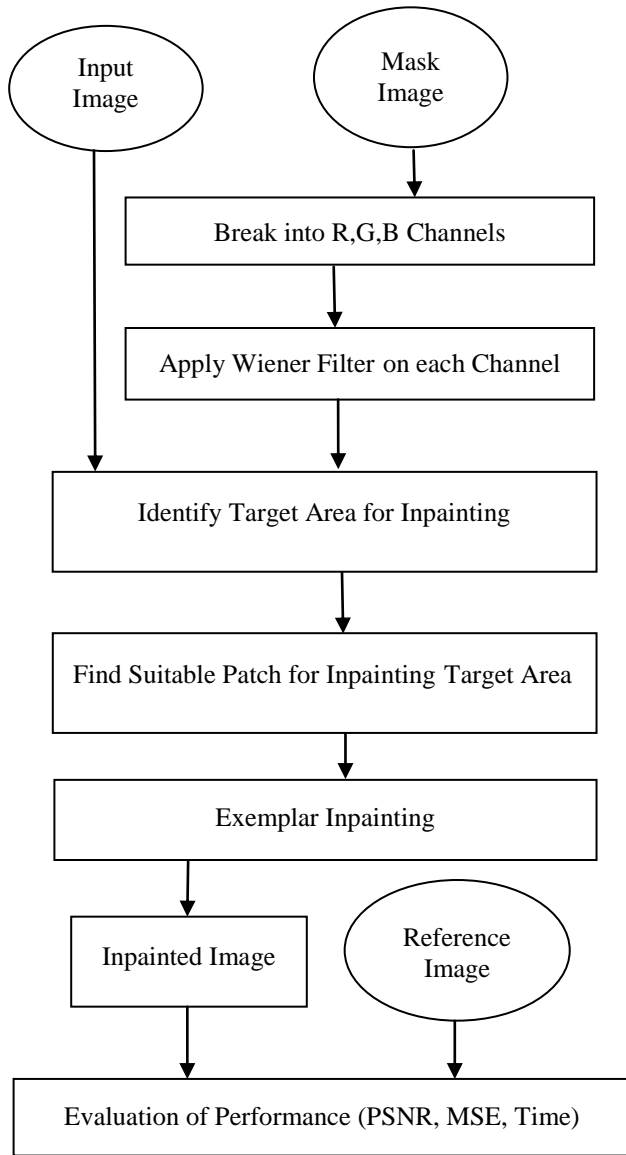


Figure 2. Flowchart of the Proposed Algorithm

Steps:

Step 1: Decompose into R, G, B Channels

The RGB mask image is broken into its component channels i.e. Red, Green and Blue.

Step 2: Apply Wiener Filter on each Channel

Wiener filtering is carried out on the mask image to filter out any noise from the mask image. This step improves the detection of the target area because it adaptively reduces the noise present in the image. The Wiener filter provides the estimates for each pixel regarding its mean and the variance locally using the equations respectively:

$$\mu = \frac{1}{NM} \sum_{n_1, n_2 \in \eta} a(n_1, n_2) \tag{1}$$

$$\sigma^2 = \frac{1}{NM} \sum_{n_1, n_2 \in \eta} a^2(n_1, n_2) - \mu^2 \tag{2}$$

η is the local neighbourhood of the pixel under consideration. This step proves very useful especially in cases where the image resizing has taken place as in such cases the marked area for inpainting gets distorted. Even the recent and sophisticated algorithms fail to handle such variations because they determine the region to be filled using a specific colour, but due to resizing or other such operations the colour used for demarcation gets merged with the surrounding pixel colours. This mixing up results in poor mask processing and hence the results produced are also affected. Wiener filtering helps to remove such types of noise from the mask thereby leading to better identification of the mask and the non-mask area.

Step 3: Identify Target Area

After filtering the next step is to perform inpainting on the identified target region. The target area is identified using the mask image and the input image. The mask image contains the manually demarcated area specifying the portion to be inpainted.

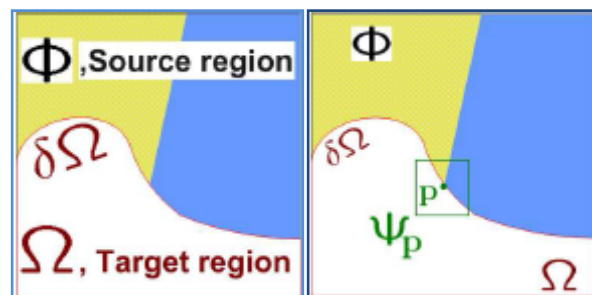
Step 4: Find Suitable Patch For Inpainting

The most suitable patch is selected by using the approach formulated by Criminsi [4]. This method has been extensively utilized and studied because this inpainting approach utilizes the benefits of texture synthesis as well as structure inpainting.

To find the best suitable patch, priorities are assigned to all the patches using the following equation:

$$P(p) = C(p)D(p) \tag{3}$$

D symbolizes the Data and C defines the Confidence term and p refers to the patch under consideration.



(a)

(b)

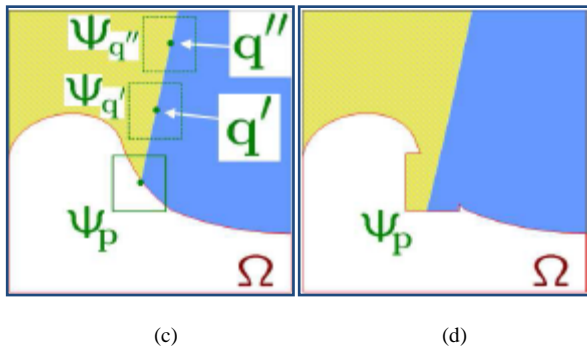


Figure 3. Filling target area by Criminisi's Algorithm [4]. (a) The source, target and fill boundary marked by ϕ , Ω and $\delta\Omega$ respectively. (b) ψ_p is the patch to be inpainted. (c) Candidate patches to be used for inpainting example $\psi_{q'}$. (d) Inpainted ψ_p .

These terms are evaluated as follows:

$$C(p) = \frac{\sum_{q \in \psi_p \cap (\Omega - \Omega)} C(q)}{|\psi_p|} \quad (4)$$

$$D(p) = \frac{|\nabla I_p^\perp \cdot n_p|}{\alpha} \quad (5)$$

where α denotes the normalization factor, $|\psi_p|$ symbolizes the patch area, n_p is unit vector perpendicular to the fill boundary $\delta\Omega$. The highest priority patch $\psi_{\hat{p}}$, another patch that matches $\psi_{\hat{q}}$ is calculated such that the dissimilarity (sum of squared difference) between the two is minimum is computed and selected as the suitable patch.

Step 5: Exemplar Inpainting

This patch selected by Step 4 is then used to inpaint $\psi_{\hat{p}}$, and the process continues for other elements in the fill boundary. After each such iteration the confidence and data terms are updated for the next round. The algorithm fills up the target area by inpainting the patches of a similar texture and structure [4] [10]. The structure too gets infused into this approach as is shown in the Figure 3. The approach lays a lot of stress on determining the filling order of the missing areas hence the patches are selected only on the basis of their priority. After all the iterations are completed the inpainted image is obtained.

Step 6: Evaluation of Results

The resultant image obtained is compared with a reference image to find out how effective the inpainting approach is. The quality metrics-MSE, PSNR, Execution time and Visual results are calculated for the test image set.

IV RESULTS AND COMPARISON

The proposed algorithm is applied to various images and the results are computed in terms of the following four quality parameters:

A. MSE (Mean Squared Error):

Metric used over every colour channel to find deviance from the reference image's respective colour channel values. These values are divided by the image size and average is taken to calculate MSE of coloured image. For any colour channel c , the MSE is calculated as:

$$MSE(c) = \frac{1}{mn} \sum_{i=0}^{m-1} \sum_{j=0}^{n-1} [I(i, j) - K(i, j)]^2 \quad (6)$$

I refers to the inpainted image, K depicts the reference image and $[m*n]$ is the size of the image. After calculating MSE for all 3 channels red green and blue- $MSE(r)$, $MSE(g)$, $MSE(b)$, Average is taken to find the overall image MSE:

$$MSE = \frac{1}{3} (MSE(r) + MSE(g) + MSE(b)) \quad (7)$$

The overall MSE results obtained by applying our approach and approach [4], [9] and [18] on set of test images are shown in the table below for comparison and analysis.

Table I. MSE comparison for different test images

Image	Exemplar [4]	Our Technique	HaLTRC [9]	HOSVD [18]
Sun (Fig. 6)	0.1218	0.0693	7.351433	0.86753
Building (Fig. 7)	0.0915	0.0715	48.76986	9.25534
Tree (Fig. 8)	0.4726	0.2392	17.0968	0.6204
Sea (Fig. 9)	0.0264	0.0239	0.1291	0.0932
Ship (Fig. 10)	0.0437	0.0353	1.3869	1.45892

Table I shows that our technique outperforms the other techniques in terms of MSE Value. It implies that our inpainted image has less mean squared error when compared to the reference image than that of inpainted images by other techniques.

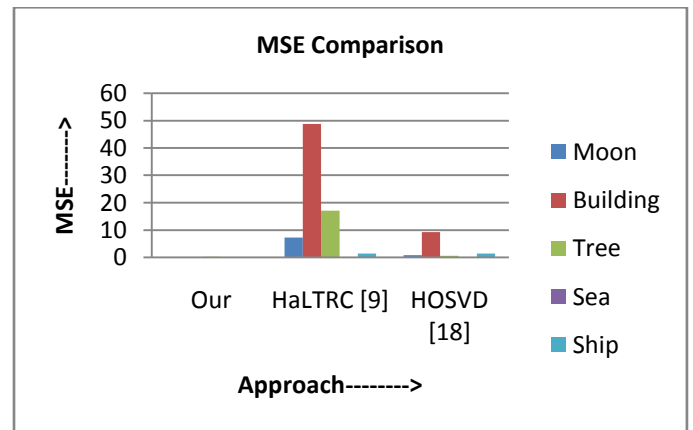


Figure 4. MSE Comparison Graph

A graph showing the MSE comparison between our technique and the techniques provided by [9] and [18] is shown in Figure 4. The x-axis shows the approach used and y-axis shows the MSE values. The key is provided wherein different test images are depicted by different colours.

B. PSNR (Peak Signal to Noise Ratio):

It provides the measure of the inpainted image quality with respect to the reference image. The higher the PSNR value, the closer the inpainted image resembles the reference image thus better the quality of the inpainted image. A poor PSNR value indicates noise in the image and deviation from the expected results.

The value is computed as an average of the PSNR values across each component channel.

$$PSNR = 10 * \log_{10} \left[\frac{255^2}{MSE} \right] \tag{8}$$

where 255 is the maximum possible intensity and MSE is overall MSE of the image.

The results obtained by applying our approach on the set of test images are shown in the table below along with the results obtained by applying [4], [9] and [18] on the same set of images. The PSNR value comparison is as follows:

Table II. PSNR comparison for different test images

Image	Exemplar [4]	Improved Exemplar	HaLTRC [9]	HOSVD [18]
Sun (Fig. 6)	57.2758	59.7245	39.46708	48.74794
Building (Fig. 7)	58.5174	59.5877	31.24929	38.46688
Tree (Fig. 8)	51.386	54.3439	35.8017	50.2043
Sea (Fig. 9)	63.9189	64.3514	57.0204	58.437
Ship (Fig. 10)	61.7301	62.6531	46.7104	46.4905

Table II clearly proves that our technique produces better results in comparison to the other techniques in terms of PSNR. It implies that our inpainted image conforms more closely to the reference (expected) image than that of inpainted images by other techniques.

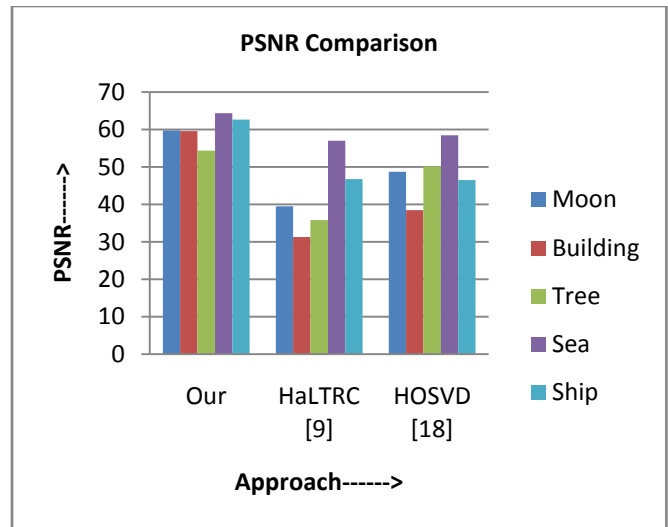


Figure 5. PSNR Comparison Graph

A graph plotted for providing a comparison between the PSNR values of our technique and the techniques provided by [9] and [18] is shown in Figure 5. The x-axis depicts the approach used and y-axis denotes the PSNR values obtained. To obtain the PSNR the inpainted image is compared to the reference image. The key is provided wherein different test images are depicted by different colours.

C. Visual Quality:

The visual quality for all the test images can be judged from the figures showing - input image, the mask image, the reference image and the inpainted image obtained by our method. The quality of the inpainted image obtained as output can be seen to be visually coherent to the reference image.

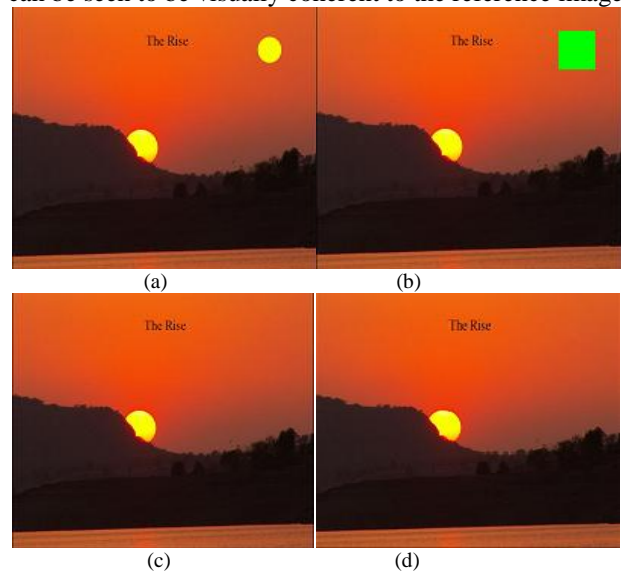


Figure 6. Sun.png (a) Input Image (b) Mask Image (c) Reference Image (d) Inpainted Image

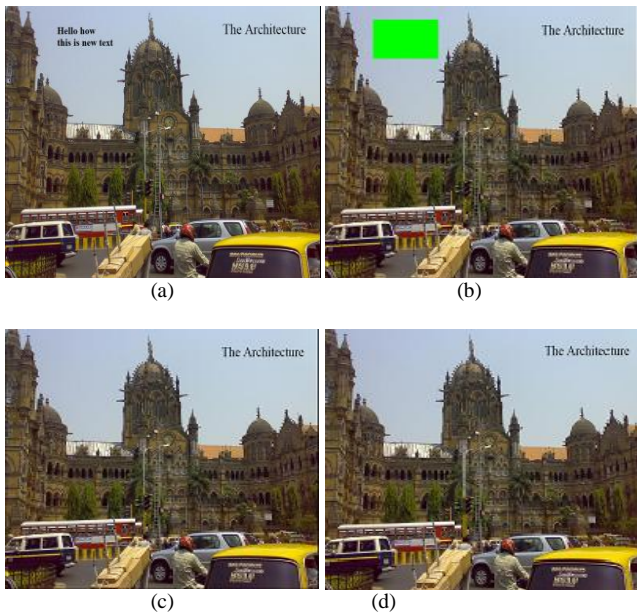


Figure 7. Building.png (a) Input Image (b) Mask Image (c) Reference Image (d) Inpainted Image

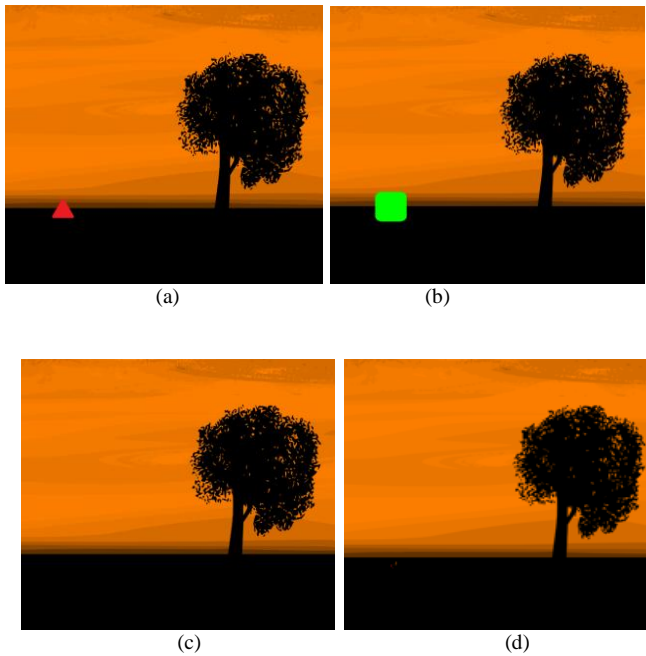


Figure 8. Tree.png (a) Input Image (b) Mask Image (c) Reference Image (d) Inpainted Image

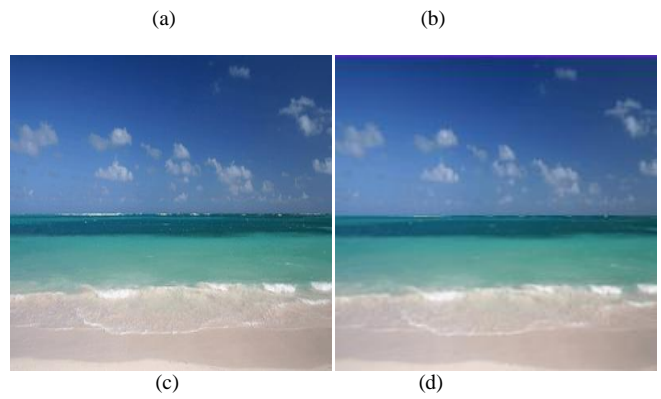


Figure 9. Sea.png (a) Input Image (b) Mask Image (c) Reference Image (d) Inpainted Image

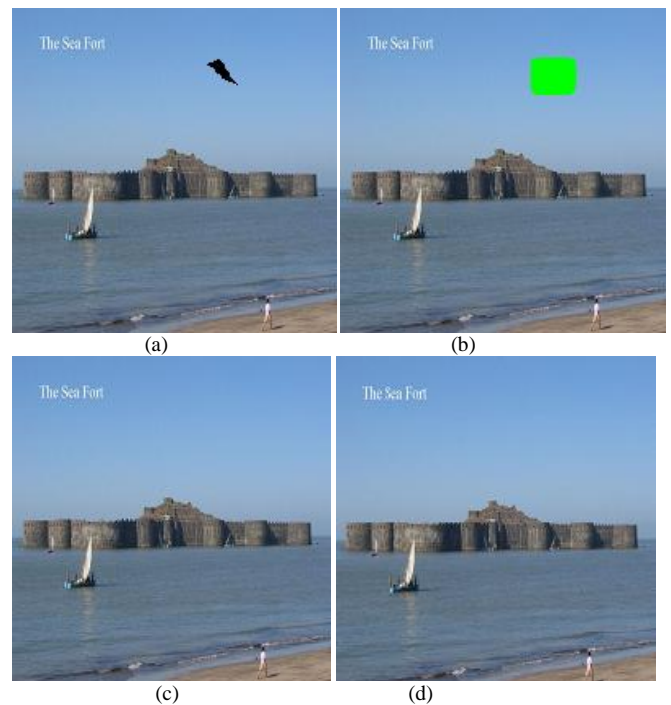


Figure 10. Ship.png (a) Input Image (b) Mask Image (c) Reference Image (d) Inpainted Image

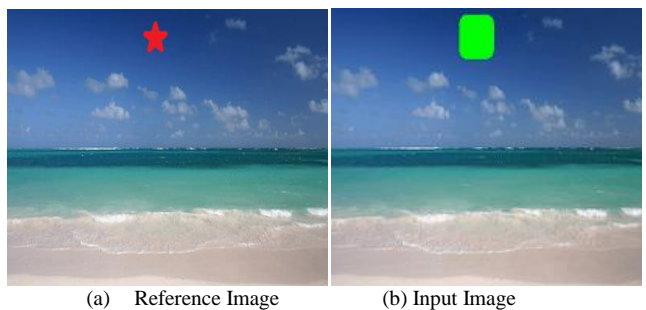
Figure 6(a) shows the input image having an extra sun which needs to be removed by the help of inpainting. The mask is created as shown in Figure 6(b) so that the reference image Figure 6(c) can be obtained. The result of applying our inpainting approach is shown in Figure 6(d). It is clear that the output resembles the reference image very closely. Similarly for Figure 7, Figure 8, Figure 9 and Figure 10 the results have been shown and can be seen to be almost identical to their respective reference images.

A comparison of the visual quality of inpainted image obtained by [9], [18] and our technique is provided for the Sun.png test image in the figure below:



Figure 11. Comparison with sun.png (a) Input Image. (b) Mask Image. (c) Reference Image (d) Inpainted Image by [9] (e) Inpainted Image by [18] (f) Inpainted Image by our technique

The results show certain marks left in the Figure 11(d) as tensor based method [9] is biased towards structure inpainting and fails to provide good results for a whole patch of missing data and is more suited for smaller missing regions. Figure 11(e) appears better but does not seem so close to the reference image as is Figure 11(f).



(a) Reference Image (b) Input Image

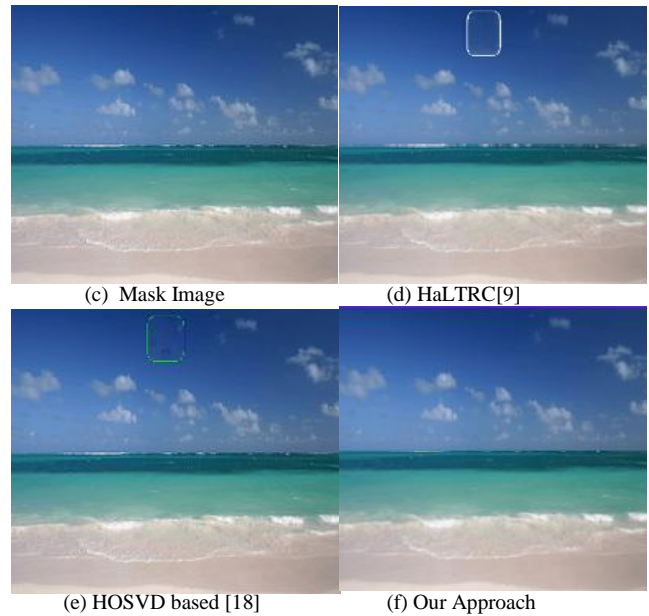


Figure 12. Comparison with sea.png (a) Input Image. (b) Mask Image. (c) Reference Image (d) Inpainted Image by [9] (e) Inpainted Image by [18] (f) Inpainted Image by our technique.

Figure 12 shows results obtained when input image, mask image and reference are scaled down from 400x250 to 200x200. The mask colours get merged with the surrounding pixels and mask processing by [9] and [18] fails in this case as outlines of the mask are visible in the inpainted image as shown in Figure 12(d) and Figure 12(e). Our approach Figure 12(f) works perfectly in this case too as the Wiener filter handles the noise produced thus mask processing is not affected.

D. Execution Time:

The execution time of the approach is calculated from the beginning of the algorithm till the end of the algorithm when the inpainted image is obtained. The results obtained for the test image set are shown in the table below:

Table III. Execution Time (in seconds)

Image	Exemplar [4]	Our Technique	HaLTRC [9]	HOSVD [18]
Sun (Fig. 6)	2.1902	1.7801	41.47997	16.90717
Building (Fig. 7)	3.9543	3.4832	38.49693	32.84791
Tree (Fig. 8)	0.9843	1.0903	27.03766	6.980575
Sea (Fig. 9)	2.7209	2.0162	25.51792	10.94332
Ship (Fig. 10)	1.8531	1.5468	14.58182	9.454139

It is clear from Table III that our technique is competitive to other methods and produces excellent results in minimum time. These observations suggest that inpainting can be done faster and more efficiently using our approach. These values have been taken on Intel Core 2.40 GHz i3 processor.

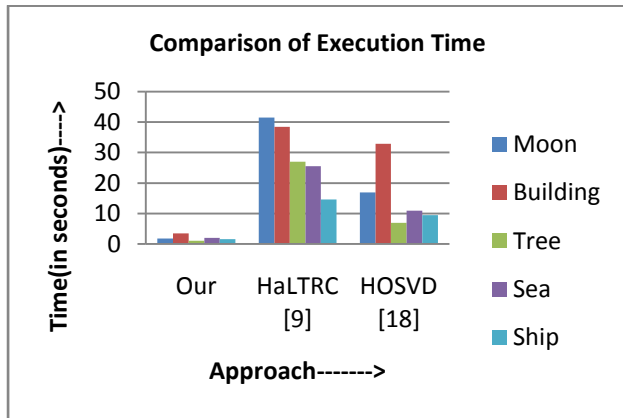


Figure 13. Comparison of Execution Time

The graph in Figure 13 shows a comparison between the execution time taken by our technique and the techniques provided by [9] and [18]. The x-axis depicts the approach used and y-axis denotes the time taken in seconds.

V CONCLUSION

The proposed algorithm works by first applying noise reduction technique to the mask image and then inpainting it. This step enables correct mask processing even in cases where image has been resized or mask not correctly demarcated. Exemplar inpainting is used for inpainting using the filtered mask image and input image. The approach yields visually high quality results and is also efficient in terms of execution time. The results show the effectiveness of the scheme. In future, we wish to work for historical images enhancement and restoration so that the treasure of knowledge held in old manuscripts, artworks and paintings can be explored.

REFERENCES

[1] M. Bertalmio, J. Sapiro, V. Caselles, et al. Image inpainting. In: Proceedings of SIGGRAPH[C], New Orleans, USA, 2000: 417-424.
 [2] Shen, Jianhong, and Tony F. Chan, 2002 "Mathematical Models For Local Nontexture Inpaintings", *SIAM J. Appl. Math.* 62.3,1019-1043.
 [3] Shen, Jianhong, Sung Ha Kang, and Tony F. Chan. 'Euler's Elastica And Curvature-Based Inpainting'. *SIAM J. Appl. Math.* 63.2 (2003): 564-592.a
 [4] Criminisi, A., P. Perez, and K. Toyama. 'Region Filling And Object Removal By Exemplar-Based Image Inpainting'. *IEEE Trans. on Image Process.* 13.9 (2004): 1200-1212
 [5] Zhu, Chuang, Huizhu Jia, Meng Li, Xiaofeng Huang, and Xiaodong Xie. "Highly Efficient Local Non-Texture Image Inpainting Based on Partial

Differential Equation." In *Computational Science and Engineering (CSE), 2014 IEEE 17th International Conference on*, pp. 803-807. IEEE, 2014.
 [6] Chan T, Shen J. Non-texture Inpainting by Curvature-Driven Diffusions(CDD) [J].*Journal of visual Communication and Image Representation*, 2001.12(4): pp436-449.
 [7] Igehy, H.; Pereira, L., "Image replacement through texture synthesis," *Image Processing, 1997. Proceedings., International Conference on Image Processing*, vol.3, no., pp.186,189 vol.3, 26-29 Oct 1997
 [8] Shih, T., Chang, R.-C., Lu, L.-C., & Ko, W.-C., "Adaptive Digital Image Inpainting". *AINA 2004. 18th International Conference on Advanced Information Networking and Applications, IEEE, 2004 (Volume:1)* (pp. 71 - 76).
 [9] Ji Liu; Musialski, P.; Wonka, P.; Jieping Ye, "Tensor Completion for Estimating Missing Values in Visual Data," *IEEE Transactions on Pattern Analysis and Machine Intelligence* , vol.35, no.1, pp.208,220, Jan. 2013
 [10] Alilou, V.K.; Yaghmaee, F., "Introducing a new fast exemplar-based inpainting algorithm," *22nd Iranian Conference on Electrical Engineering (ICEE), 2014*, vol., no., pp.874,878, 20-22 May 2014
 [11] Guillemot, C.; Turkan, M.; Le Meur, O.; Ebdelli, M., "Image inpainting using LLE-LDNR and linear subspace mappings", *IEEE International Conference on Acoustics, Speech and Signal Processing (ICASSP)*, vol., no., pp.1558,1562, 26-31 May 2013
 [12] Li, Q., Han, Y., & Dang, J. "Image decomposing for inpainting using compressed sensing in DCT domain", *2014 Frontiers of Computer Science, Volume 8, Issue 6*, pp 905-915, 905-915.
 [13] Chen, Weihai et al. "An Improved Edge Detection Algorithm For Depth Map Inpainting", 2014, *Optics and Lasers in Engineering* 55:69-77.
 [14] Guillemot, C.; Le Meur, O., "Image Inpainting : Overview and Recent Advances," *Signal Processing Magazine, IEEE* , vol.31, no.1, pp.127,144, Jan. 2014
 [15] Shin, Seunghyup, Tomoyuki Nishita, and Sung Yong Shin. 'On Pixel-Based Texture Synthesis By Non-Parametric Sampling'. *Computers & Graphics* 30.5 (2006): 767-778.
 [16] Zhen Xie; Fan Zhang; Conggui Zhang, "An adaptive matching algorithm for image inpainting," *2011 International Conference on Electronics, Communications and Control (ICECC)*, vol., no., pp.1293,1296, 9-11 Sept. 2011
 [17] M. Bertalmio, L. Vese, G. Sapiro, and S. Osher, "Simultaneous structure and texture image inpainting," *IEEE Transactions on Image Processing*, Vol. 12, 2003, pp. 882-889.
 [18] Ghorai, M.; Chanda, B., "An Image Inpainting Algorithm Using Higher Order Singular Value Decomposition," *22nd International Conference on Pattern Recognition (ICPR)*, vol., no., pp.2867,2872, 24-28 Aug. 2014
 [19] J. Sun, L. Yuan, J. Jia, and H. Y. Shum, "Image completion with structure propagation," in Proceedings of SIGGRAPH, 2005, pp. 861-868.
 [20] W. Cheng, C. Hsieh, S. Lin, C. Wang, and J. Wu, "Robust algorithm for exemplar based image inpainting," in Proceedings of International Conference on Computer Graphics, Imaging and Visualization, 2005, pp. 64-69.
 [21] Zongben Xu, and Jian Sun. 'Image Inpainting By Patch Propagation Using Patch Sparsity'. *IEEE Trans. on Image Process.* 19.5 (2010): 1153-1165.
 [22] Yongsheng Xu; Shuwen Wang, "Image inpainting based on wavelet transformation," *5th IEEE International Conference on Software Engineering and Service Science (ICSESS)*, vol., no., pp.541,544, 27-29 June 2014
 [23] Vahid Bastani, M. S. "Image compression based on spatial redundancy removal and image inpainting", 2010, *Journal of Zhejiang University SCIENCE C, Volume 11, Issue 2*, 92-100

[24] Awate, S.P.; Whitaker, R.T., "Unsupervised, information-theoretic, adaptive image filtering for image restoration," *Pattern Analysis and Machine Intelligence, IEEE Transactions on Pattern Analysis and Machine Intelligence (TPAMI)*, vol.28, no.3, pp.364,376, March 2006
[25] Aurélie Bugeau, Marcelo Bertalmio, Vicent Caselles, Member, IEEE, and Guillermo Sapiro, "A Comprehensive Framework for Image Inpainting", *IEEE transactions on Image Processing*, vol. 19, no. 10, pp. 2634-2645, MAY 2010.

Authors Profile



Lavina Kalra is currently pursuing Regular M.E. in Computer Science & Engineering from National Institute of Technical Teachers Training and Research (NITTTR), Chandigarh, India. She has completed her B.E. from Panjab University Swami Sarvanand Giri Regional Centre, Hoshiarpur.



Dr. Maitreyee Dutta is currently working as Professor and Head in Electronics and Communication Engineering Department of National Institute of Technical Teachers Training & Research, Chandigarh, India. Former she was professor and Head in Computer Science Department of National Institute of Technical Teachers and Training Research (NITTTR), India. She completed her B.E. from Gauhati University and M.E. from PEC University of technology. Her research area is Digital Image Processing, Digital Signal Processing, Data Warehousing and Data Mining etc.